A Comparison between the Stereoselective Thermal-Induced and Ionization-Induced Elimination of Acetic Acid from 2-Butyl Acetate

Mark M. Green,*[1a] Richard J. McCluskey,[1b] and Jürgen Vogt[1c]

Contribution from the Department of Chemistry, Polytechnic Institute of New York, Brooklyn, New York 11201, Department of Chemical Engineering, Clarkson College, Potsdam, New York 13676, and Physikalisch Chemisches Institut der Universität Basel, 4056 Basel, Switzerland. *Received July 27, 1981*

Abstract: Photoelectron photoion coincidence spectrometry shows that the ionized acetate ester of *sec*-butyl alcohol eliminates acetic acid just above the ionization potential but cleaves to form $C_2H_3O^+$ at energies greater than 2 eV above this point. Experiments with the C-3 deuterium-labeled diastereomers of 2-butyl acetate show the elimination reaction to be stereoselective at all energies 0.1 eV greater than the ionization potential. These measurements were made by threshold photoelectron photoion coincidence spectrometry (TPEPICO). The TPEPICO stereoselective channel ratios were fit well by RRKM calculations in which the threshold energy difference for the stereoisomeric pathways was 600–800 cal/mol. These numbers may be minimum values if a C-3 epimerization, i.e., stereochemical scrambling, mechanism intervenes in these ions. Such a process is probably responsible for the absence of stereoselection in the metastable ions formed in an electron-impact mass spectrometer. Published data on the thermal decomposition of 2-butyl acetate imply a difference in threshold energy for the stereochemical paths of 690–830 cal/mol. Existing mechanistic proposals for the loss of acetic acid from the ion (McLafferty rearrangement) and from the neutral suggest similar threshold energy differences for the stereoselective pathways. Integration of the microscopic stereoselective channel ratios over the PEPICO-derived energy distribution function of those molecular ions which undergo elimination of acetic acid predicts the photoionization source temperature dependence of the stereoselectivity should be less than that experimentally observed in an electron-impact mass spectrometer.

The acetate ester of *sec*-butyl alcohol on activation by ultraviolet irradiation, ionization, or heating is known to decompose to acetic acid and the various C_4H_8 isomers.[2] Under the conditions of the heat initiated reaction, e.g., 673 K, precise kinetic work[3-5] shows the Arrhenius energy of activation to be 2 eV and the products to be 1-butene, *cis*-2-butene, and *trans*-2-butene with the stereoisomers formed in a trans/cis ratio of 1.86/1 via a kinetically controlled stereospecific cis elimination.[6]

The electron impact mass spectrum of 2-butyl acetate taken at a beam energy a few volts above the ionization threshold is exhibited in Figure 1. The ion at m/e 56 has the elemental composition $C_4H_8^{+\cdot}$ arises via the loss of acetic acid directly from the molecular ion and has an appearance potential near to the molecular ionization potential.[7,8] This is consistent with thermochemical estimation of the heat of reaction for forming $C_4H_8^{+\cdot}$ from 2-butyl acetate using the following heats of formation (ΔH_f): 2-butyl acetate (−500.8 kJ/mol); acetic acid (−432.2 kJ/mol); $C_4H_8^{+\cdot}$ (871 kJ/mol).[9,10]

In a parallel experiment to the determination of the stereochemistry of the thermal reaction the two known[6] diasteromers incorporating deuterium for each of the diastereotopic hydrogens at C-3 in 2-butyl acetate (**1** and **2**, see Figure 6 below) have been subjected to electron-impact ionization at varying temperatures of the source and at electron beam energies of 70 eV and at near the beam energy utilized in Figure 1. Because the isotope effect in the ion reaction (kH/kD)[11,12] is near unity, the ratio of deuterated acetic acid loss to all acetic acid loss from each diastereomer (**1** and **2**) yields the stereoselectivity (designated $\bar{k}_a/\bar{k}_b$) for the loss of the diastereotopic hydrogens at C-3 in 2-butyl acetate.[8] This stereoselectivity has been shown to be greater than one and to be strongly dependent on source temperature, yielding a straight line in a plot of $\ln(\bar{k}_a/\bar{k}_b)$ vs. the inverse absolute temperature of the ion source.[13] The greater loss of deuterated acetic acid from **1** over **2** is consistent with the heat-initiated reaction.[6] The quantitative relationship between the stereoselectivities in the compared reactions, i.e., 1.86/1 at 673 K[6] and 1.68/1 at 70 eV and 312 K,[13] is a subject of interest.

Using procedures to be discussed below, the Boltzmann distribution of vibrational energies for 2-butyl acetate at 673 K has been calculated (Figure 2) and, because above 2 eV on the energy axis the neutral molecules are active enough to eliminate acetic acid,[5] we can precisely define the energy states responsible for the stereochemistry observed.[6]

In the ion produced by electron impact, there is only an approximate knowledge of the population of energy states responsible for the chemical observations. Instrumental advances however supply this important information for ionization by photons. In the present work we have inspected the details of loss of acetic acid from 2-butyl acetate ionized by photons. If we can learn the energetic basis for the ion chemistry of 2-butyl acetate, we can begin to understand its relationship to the heat-initiated chemistry of this molecule.

Results

In the photoelectron photoion coincidence (PEPICO) experiment a photoelectron spectrometer and a mass spectrometer are

(1) (a) Polytechnic Institute of New York. (b) Clarkson College. (c) Physikalisch Chemisches Institut der Universitat Basel.
(2) W. H. Saunders and A. F. Cockerill, "Mechanisms of Elimination Reactions", Wiley-Interscience, New York, 1973, p 406 ff; 615 ff.
(3) E. U. Emovon and A. Maccoll, *J. Chem. Soc.*, 335 (1962).
(4) J. C. Scheer, E. C. Kooyman, and F. L. J. Sixma, *Rec. Trav. Chim. Pays-Bas*, **82**, 1123 (1963).
(5) S. W. Benson and H. E. O'Neal, *Natl. Stand. Ref. Data Ser. (U.S. Natl. Bur. Stand.)*, **21**, 170 (1970). See also pages 12–14 and 23–36.
(6) P. S. Skell and W. L. Hall, *J. Am. Chem. Soc.*, **86**, 1557 (1964).
(7) J. H. Beynon, R. A. Saunders, and A. E. Williams, *Anal. Chem.*, **33**, 221 (1961).
(8) M. M. Green, J. M. Moldowan, D. J. Hart, and J. M. Krakower, *J. Am. Chem. Soc.*, **92**, 3491 (1970); M. M. Green, J. M. Moldowan, and J. G. McGrew, II, *J. Org. Chem.*, **39**, 2166 (1974). The metastable and high resolution measurements[7] were reproduced by Dr. E. White V. of the National Bureau of Standards. See also Figure 3.
(9) H. M. Rosenstock, K. Draxl, B. W. Steiner, and J. T. Herron, *J. Phys. Chem. Ref. Data*, **6**, Suppl. 1 (1977).
(10) S. W. Benson, F. R. Cruickshank, D. M. Goldon, G. R. Haugen, H. E. O'Neal, A. S. Rodgers, R. Shaw, and R. Walsh, *Chem. Rev.*, **69**, 279 (1969).
(11) J. K. MacLeod and C. Djerassi, *J. Am. Chem. Soc.*, **89**, 5182 (1967).
(12) M. M. Green, G. J. Mayotte, L. Meites, and D. Forsyth, *J. Am. Chem. Soc.*, **102**, 1464 (1980).
(13) M. M. Green, T. J. Mangner, S. P. Turner, and F. J. Brown, *J. Am. Chem. Soc.*, **98**, 7082 (1976).

0002-7863/82/1504-2262$01.25/0

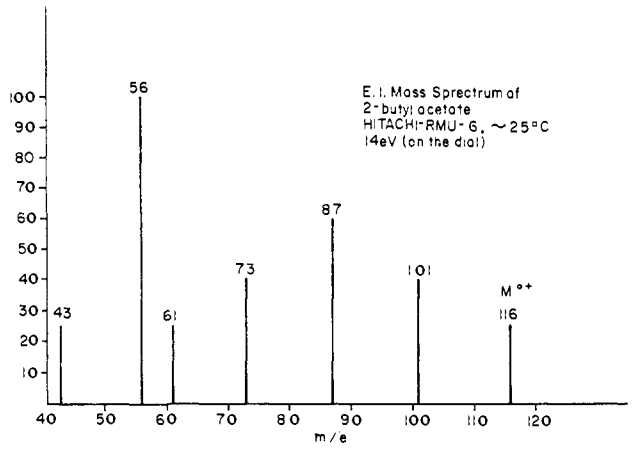

Figure 1. Electron-impact mass spectrum (C-13 corrected) of 2-butyl acetate taken on a Hitachi-RMU-6L mass spectrometer at ambient source temperature and 14-eV nominal beam energy.

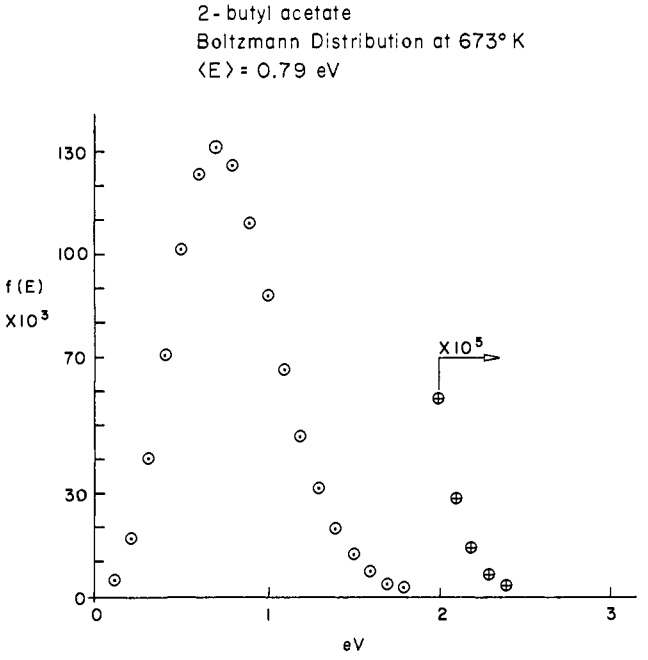

Figure 2. Boltzmann vibrational energy distribution of 2-butyl acetate at 673 K. See the text and Figure 9.

coupled[14] so that the energy of an electron emitted on ionization of a molecule by a high-energy photon can be determined in near time coincidence with the measurement of the mass of the ionic product(s) of that ionization event. In a variation of this experiment detecting, only threshold electrons or TPEPICO the photon energy is varied by utilizing an appropriate monochromator.[15] In either manner, the internal energies of all molecular ions which produce any fragment become known.

In this work 2-butyl acetate is the subject of analysis by both PEPICO and TPEPICO spectrometry. In addition, the various deuterated derivatives, **1**, **2**, and 3,3-dideuterio-2-butyl acetate

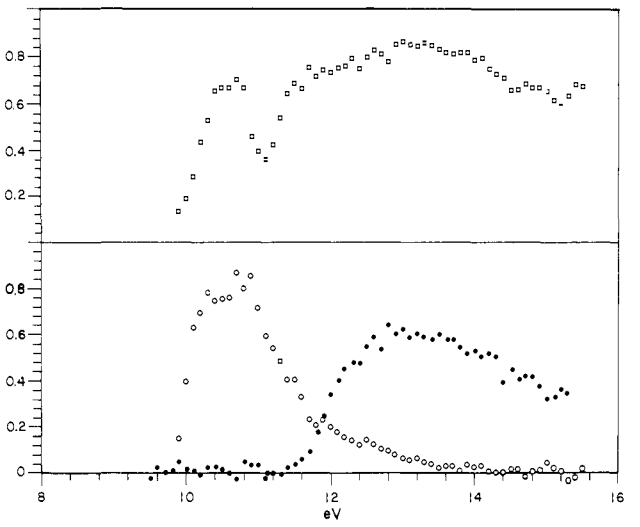

Figure 3. Top: He Iα photoelectron spectrum of 2-butyl acetate. Bottom: breakdown graphs for m/e 56 and 43 from 2-butyl acetate measured by PEPICO spectrometry. Both curves share the same abscissa which is He Iα photon energy minus the electron energy. The top ordinate represents the normalized ion population at each energy. The bottom ordinate designates the fraction of counts normalized to the photoelectron counts at the energy in coincidence with m/e 56 (○) and 43 (●) at each energy.

(**3**) have been subjected to TPEPICO analysis.

In the PEPICO experiment reported herein, the ionization wavelength is fixed at the He Iα line. Photoelectrons and photoions are accelerated in opposite directions by a weak field (4.35 V/cm) into a 127° cylindrical electrostatic analyzer and a quadrupole mass spectrometer, respectively. The electron energy resolution, and therefore also the ion internal energy resolution, was 0.1 eV (fwhm). Electron and ion collection efficiencies were $f_e \approx 10^{-4}$ and $f_i \approx 0.3$, respectively. Breakdown curves are measurements of the electron counts in coincidence with the ion of interest, e.g., m/e 56, normalized to the total electron counts at that energy, and thus graphically illustrate the probability of dissociation into a specific product ion as a function of parent ion internal energy. The PEPICO spectrometer utilized in this work has been described.[16]

The breakdown curves for m/e 56 and m/e 43 produced from He Iα photoionized 2-butyl acetate and the He Iα photoelectron spectrum (PES) of 2-butyl acetate are presented in Figure 3. The PES (figure 3 (top)) is almost identical with the isomeric *n*-butyl acetate previously measured.[17] The leading photoelectron band up to the gap at ca. 11.1 eV has been assigned to ionizations from the carbonyl oxygen lone electron pair and the essentially nonbonding antisymmetric π orbital located on the O–C–O system.[17] Although our attention is focused on the $C_4H_8^{+\cdot}$ ion at m/e 56, the ion at m/e 43 forms an effective counterpoint (Figure 3). When produced by electron impact, it is uniquely composed of $C_2H_3O^+$ and being characteristic of acetates has been assigned to simple bond cleavage of the carbonyl to oxygen bond.[18] In agreement with this hypothesis[18] we have observed in an electron-impact mass spectrometer a collisional dissociation corresponding to the transition m/e 116 → m/e 43.[19]

The two classes of unimolecular reactions represented by the product ions at m/e 56 and 43 are, respectively, rearrangement of the six-center molecular elimination type and simple bond fission[5] and therefore are expected to be most competitive from low- and high-energy molecular ions, respectively. The data in

(14) B. Brehm and E. von Puttkamer, *Z. Naturforsch., A, 22a*, 8 (1967); *Adv. Mass Spectrom.*, **4**, 591 (1968); J. H. D. Eland, *Int. J. Mass. Spec. Ion Phys.*, *8*, 143 (1972); C. J. Danby and J. H. D. Eland, *ibid.*, 153 (1972). See also J. H. D. Eland, "Specialist Periodical Reports, Mass Spectrometry", Vol. 5, The Chemical Society, London, 1979, Chapter 3. H. M. Rosenstock, R. Stockbauer, and A. C. Parr, *J. Chem. Phys.*, **71**, 3708 (1979); A. S. Werner and T. Baer, *ibid.*, **62**, 2900 (1975); C. F. Batten, J. A. Taylor, and G. G. Meisel, *ibid.*, *65*, 3316 (1976); R. Stockbauer and M. G. Inghram, *ibid.*, *62*, 4862 (1975); T. Baer in "Gas Phase Ion Chemistry", Vol. I, M. Bowers, Ed., Academic Press, New York, 1979, Chapter 5, p 153 ff.

(15) See A. C. Parr, A. J. Jason, and R. Stockbauer, *Int. J. Mass Spectrom. Ion Phys.*, **33**, 243 (1980) for leading references to this technique and to the TPEPICO spectrometer at the National Bureau of Standards utilized in this work.

(16) J. Dannacher and J. Vogt, *Helv. Chim. Acta*, **61**, 361 (1978).

(17) D. A. Sweigart and D. W. Turner, *J. Am. Chem. Soc.*, **94**, 5592 (1972).

(18) The fragmentation mechanism of 2-butyl acetate is discussed in: F. W. McLafferty, "Interpretation of Mass Spectra", 3rd ed., University Science Books, 1980, pp 202–205.

(19) Unpublished observations by Dr. E. White V. at the National Bureau of Standards.

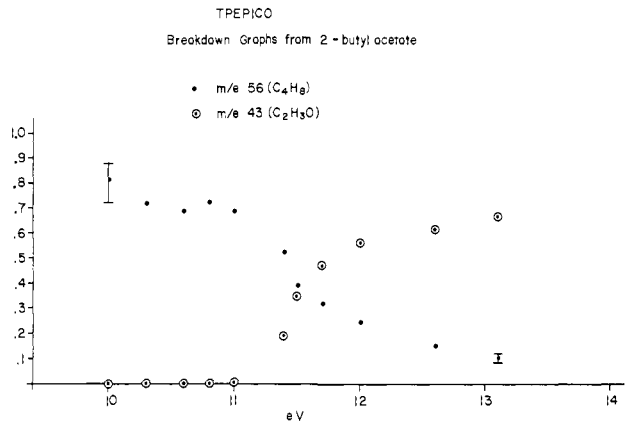

Figure 4. Breakdown graphs for m/e 56 (●) and 43 (⊙) from 2-butyl acetate measured by TPEPICO spectrometry. Axes are threshold electron counts in coincidence with each ion at each photon energy normalized to total threshold electron counts for all detected ions. Error bars show ±10% of counts and are intermediate between these values.

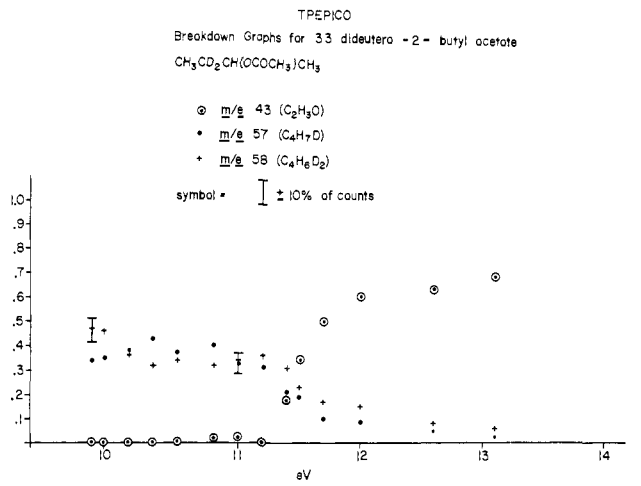

Figure 5. Breakdown graphs for m/e 57 (●), m/e 58 (+), and m/e 43 (⊙) from C-3 dideuterio-2-butyl acetate measured by TPEPICO spectrometry. See Figure 4 caption for explanation of axes.

Figure 3 confirm this prediction and are consistent with a large experimental literature showing the relationship between unimolecular reaction class[5] and internal energy.[20,21]

The breakdown graph for m/e 56 (Figure 3 (bottom)), exhibiting an onset near to the adiabatic ionization potential, is consistent with the thermochemical calculation and the low appearance energy measured in an electron-impact mass spectrometer. The theoretical and experimental work on the relationship between high-energy electron and photon ionization[22] leads to the expectation that one can expect a qualitative but not quantitative correspondence between these phenomena.

The threshold photoelectron photoion coincidence (TPEPICO, see above) spectrometry derived breakdown graphs for 2-butyl acetate and its deuterated derivatives, **1**, **2**, and **3**, discussed below, provide further insight into this system. In Figure 4 is exhibited such breakdown graphs for m/e 56 and 43 from 2-butyl acetate. Comparison with the PEPICO data in Figure 3 shows that the plateau between 10 and 11 eV and the fall off for m/e 56 are closely matched in the two breakdown graphs (m/e 56, Figures 3 and 4). Moreover, the two systems also reach close to the same fraction of concident counts for m/e 43 above 12 eV. The graphs though show substantial differences in the shape of the onset for both m/e 56 and m/e 43. For m/e 56, this difference probably arises from the TPEPICO spectrometer not allowing the precise measurement of the m/e 56, 57, and 58 ions and the molecular ion (m/e 116) simultaneously, and, since the normalization involves the counts for ions detected, the low-energy fall off observed in the Basel data (Figure 3) could not be seen in the TPEPICO device. In the former technique, the counts in coincidence with any ion are normalized to the photoelectron spectrum at that energy and the mass range incorporates the entire mass spectrum. The presence of the molecular ion can be detected in the EI mass spectrum at all ionizing energies which strongly suggests it should take an increasing fraction of the counts near the IP and thus reduce m/e 56. Breakdown graphs determined by coincidence techniques are extremely sensitive to instrument function and, in particular, to the energy resolution and the time scale for fragmentation. These factors are most important near the onset of energy for fragmentation.[23] We have not explored further these differences. The deuterated materials were all measured by threshold coincidence spectrometry[15,24] as reported below.

The breakdown graphs from 3,3-dideuterio-2-butyl acetate (**3**) and from the deuterated stereoisomers **1** and **2** for loss of HO_2CCH_3 and DO_2CCH_3 from the respective molecular ions and for m/e 43 are presented in Figures 5 and 6.

Inspection of Figure 5 shows that the breakdown curve for m/e 43 is unaffected by deuteration at carbon 3. This is consistent with the data in Figure 6 which show excellent correspondence for this ion with the undeuterated parent (Figure 4). One notes also that the ions corresponding to loss of acetic acid now appear at m/e 57 and 58. These ions reveal in turn, in the undeuterated molecule, elimination of acetic acid involving hydrogen at carbon 3 and hydrogen at all other positions, designated k_a and k_b from C-3 and k_i for all other sources of hydrogen which form acetic acid. The ratio of the areas under m/e 58 and 57 in Figure 5 has been estimated graphically to be $(1.34 \pm 0.1)/1$, and this number makes an interesting comparison to the value of $(1.20 \pm 0.1)/1$ measured for the intensities of the m/e 58 and 57 ions in the 70-eV electron-impact mass spectrum.[8] These numbers measure the ratio $k_i(k_a + k_b)$ and are similar considering the different instruments and methods of ionization used in their measurement.

The molecular symmetry allows that only acetic acid loss from the acetoxy group and a hydrogen from C-3 can be stereoselective, and this question is addressed by the experimental data in Figure 6. In the monodeuterio compounds **1** and **2** the ion at m/e 56 arises via the process represented by k_a and k_b, respectively. The breakdown graph for this ion shows it to be more intensely formed from **1** than from **2** at all photon energies which allow acetic acid loss (Figure 6). The behavior for the m/e 57 breakdown graph clearly mirrors this result, and overall, the observations are qualitatively consistent with the electron-impact observations.[8,13] The quantitative quality of the data may be judged by the demand that the sum of the ratios m/e 56/(m/e 56 + m/e 57) in **1** + m/e 56/(m/e 56 + m/e 57) in **2** + m/e 58/(m/e 57 + m/e 58) in **3** are, following from the near unity isotope effect,[11,12] equivalent

(20) These ideas are well discussed in I. Howe, D. H. Williams, and R. D. Bowen, "Mass Spectrometry", 2nd ed., McGraw-Hill, London, 1981, Chapter 3. F. W. McLafferty, "Interpretation of Mass Spectra", 3rd ed., University Science Books, 1980, Chapter 7. The earliest discussion may be found in "Electron Impact Phenomena", by F. H. Field and J. L. Franklin, Academic Press, New York, 1957, p 79.

(21) For the most recent technique see A. R. Hubik, P. H. Hemberger, J. A. Laramée, and R. G. Cooks, *J. Am. Chem. Soc.*, **102**, 3997 (1980).

(22) K. Levsen, "Fundamental Aspects of Organic Mass Spectrometry", Verlag Chemie, New York, 1978, p 12–17 and references therein. G. G. Meisels, C. T. Chen, B. G. Giessner, and R. H. Emmel, *J. Chem. Phys.*, **56**, 793 (1972); G. G. Meisels and R. H. Emmel, *Int. J. Mass Spectrom. Ion Phys.*, **11**, 455 (1973); B. N. McMaster, "Specialist Periodical Reports, Mass Spectrometry", Vol. 3, The Chemical Society, London, 1975, pp 10–14 and numerous references therein. For related discussions see A. Katrib, T. P. Debies, R. J. Colton, T. H. Lee, and J. W. Rabalais, *Chem. Phys. Lett.*, **22**, 196 (1973); S. Trajmar, *Acc. Chem. Res.*, **13**, 14 (1980) and references therein; M. Okuti, *Rev. Mod. Phys.*, **43**, 297 (1971); W. C. Tam and C. E. Brion, *J. Electron Spectrosc. Relat. Phenom.*, **3**, 467 (1974); *ibid.*, **4**, 139 (1974).

(23) An especially instructive account of these effects is found in R. Stockbauer and H. M. Rosenstock, *Int. J. Mass Spectrom. Ion Phys.*, **27**, 185 (1978).

(24) Recent papers utilizing TPEPICO with leading references are A. C. Parr, A. J. Jason, R. Stockbauer, and K. E. McCulloh, *Int. J. Mass. Spectrom. Ion. Phys.*, *30*, 319 (1979); H. M. Rosenstock, R. Stockbauer, and A. C. Parr, *J. Chem. Phys.*, **71**, 3708 (1979); *ibid.*, **73**, 773 (1980).

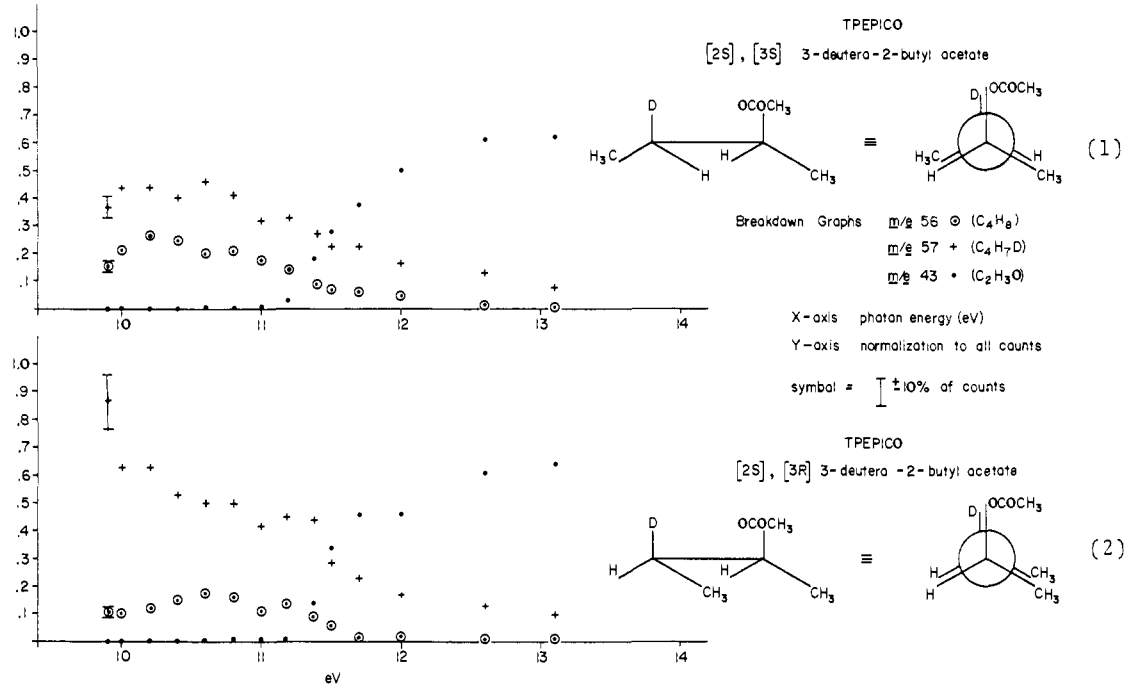

Figure 6. Breakdown graphs from **1** (top) and **2** (bottom). See caption for Figure 4.

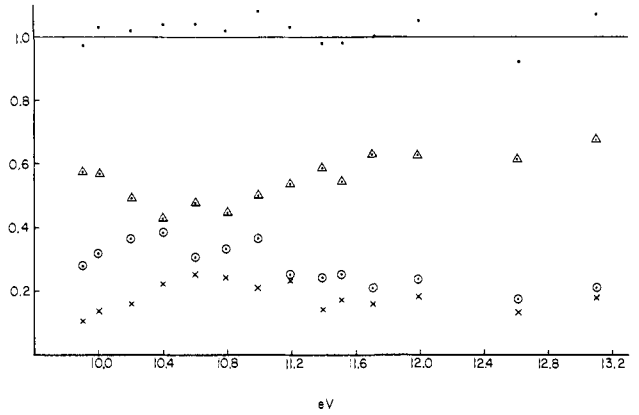

Figure 7. TPEPICO data: abscissa, photon energy; ordinate, fraction of electron counts for m/e values as follows: (△) 58/(57 + 58) (**3**); (⊙) 56/(56 + 57) (**1**); (×) 56/(56 + 57) (**2**); (•) sum at each photon energy. See text.

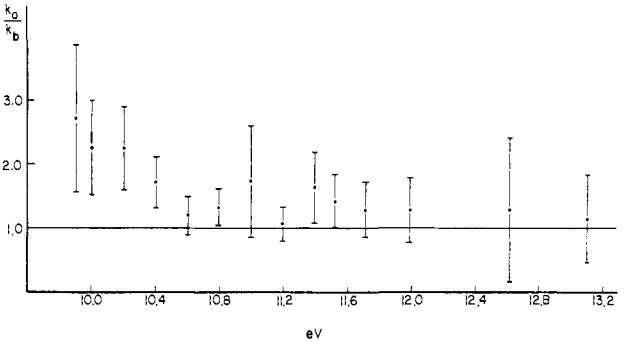

Figure 8. TPEPICO-derived microscopic stereoselective channel ratios for loss of acetic acid from 2-butyl acetate ion. The abscissa is the photon energy. The data were taken at room temperature. See text for further explanation and error analysis.

to the sum $k_a/(k_a + k_b + k_i) + k_b/(k_a + k_b + k_i) + k_i/(k_a + k_b + k_i)$ and therefore must equal unity. Figure 7 presents the results of this test of the data in Figures 4–6.

The breakdown graphs for m/e 56 and 57 from **1** and **2** may be treated so as to yield the k_a/k_b ratios at the known internal energies defined by the x axis in Figure 6, i.e., the microscopic stereoselective channel ratios. The error in these values may be judged by the results in Figure 7. At each energy the variance of the sum of the ion mass ratios about one was used as a measure of the experimental error. The variance of the ion mass ratio was taken as one third the variance of the sum. The stereoselective channel ratios for each energy (k_a/k_b) were found by dividing the ratio of counts in coincidence with m/e 56/(m/e 56 + m/e 57) from **1** by the corresponding ratio from **2**. These channel ratios are plotted vs. energy in Figure 8 and show, with some scatter, a general decrease as energy increases. The error bars illustrate ±2 standard deviations, i.e., twice the square root of the variance for the quotient of mass ratios. In determining the error limits, the variance for the ion mass ratios was taken as the larger of either the variance at the particular deposition energy or the average variance for the 12 lowest energies.

If the HOAc elimination reaction were entirely due to McLafferty rearrangements, k_i would be the microscopic rate constant for reaction involving C-1 hydrogen and $k_i/(k_a + k_b + k_i)$ would increase monotonically with energy while $k_a/(k_a + k_b + k_i)$ would show a monotonic decrease. Such monotonicity is evident in Figure 7 only for energies beyond 0.8 eV. The increase of k_i at the lowest energy suggests that more than one process contributes to this term. This is consistent with observations in electron-impact and photon ionization mass spectrometry which show there is a loss of acetic acid involving hydrogen on the δ-carbon, i.e., C-4 in 2-butyl acetate.[25]

The value of $\bar{k}_a/\bar{k}_b$ determined in the TPEPICO experiment (Figure 6) weighed over all energies can be obtained by simply taking the ratio of the areas under the breakdown graph for m/e 56 from **1** and **2**. This procedure yields the value (1.51 ± 0.1)/1. It is interesting to compare this value to the 312 K inlet temperature value of (1.68 ± 0.05)/1 for $\bar{k}_a/\bar{k}_b$ measured by electron-impact mass spectrometry.[13]

In the work below we have concentrated on the photon ionization process and developed a model for the energy distribution of the molecular ions, yielding m/e 56. With this knowledge in place, we first attempted to theoretically understand how temperature would affect the stereoselectivity of the elimination from the ion in order to shed light on the temperature sensitivity of the electron-impact results.[13] We then went on to develop RRKM models for the loss of acetic acid from 2-butyl acetate on photon

(25) W. Benz and K. Biemann, *J. Am. Chem. Soc.*, **86**, 2375 (1964); W. S. Briggs and C. Djerassi, *J. Org. Chem.*, **33**, 1612 (1968).

Table I. Fundamental Frequencies and Density of States ($N(E)$) for 2-Butyl Acetate

fundamental freq of 2-butyl acetate, cm^{-1}	energy, cm^{-1}	$N(E)$
202	2000	24
252		
281	4000	7.56×10^3
335		
353	6000	6.71×10^5
400		
418	8000	3.34×10^7
444		
454	10000	1.08×10^9
478		
658	12000	2.50×10^{10}
860		
894	14000	4.50×10^{11}
940		
972		
1020		
1030 (4)		
1100 (2)		
1110		
1120		
1250 (3)		
1370 (5)		
1470 (8)		
1720		
1763		
2940 (12)		

ionization and on heating. Comparisons of the models with our experimental data would give insight to the relationship between the reaction of the ion and of the neutral molecule.

The Energy Distribution Function for 2-Butyl Acetate Ions Which Eliminate Acetic Acid. The convolution integral (eq 1)

$$F(E) = \int_0^E D(y)P(E-y)_e \, dy \qquad (1)$$

allows the calculation of the total energy distribution function $F(E)$ for molecular ions produced from an array of thermal molecules with a Boltzmann distribution $P(E)$ and with an energy deposition function for the ionization of $D(y)$.[26] The molecular ions will be isolated from all collisions after the ionization event and the assumptions are made that all forms of energy are randomized intramolecularly and that the ionization process does not distort the distribution of thermal energy originally present in the neutral. In this integral $P(E-y)_e$ represents the appropriate thermal energy distribution for the neutral temperature shifted along the energy axis so that zero corresponds to the adiabatic ionization potential. $D(y)$, the ionization deposition function, is then taken to be the He Iα photoelectron spectrum (Figure 3).

The Boltzmann distributions of vibrational energy for 2-butyl acetate at various temperatures of interest were calculated from the fundamental frequencies of 2-butyl acetate available in the literature.[27] These were modeled as harmonic oscillators and are listed in Table I. The density of states functions, $N(E)$, was calculated from the frequencies using the direct count algorithm of Beyer and Swinehart.[28] The energy distributions were discretized. $P(E)$, the Boltzmann distribution, represents the fraction of energy states within ±0.05 eV of energy E and was computed by appropriately summing the $P(E)$ Boltzmann equation. These calculations were performed to where the magnitude of $P(E)$ was 10^{-5} or less.

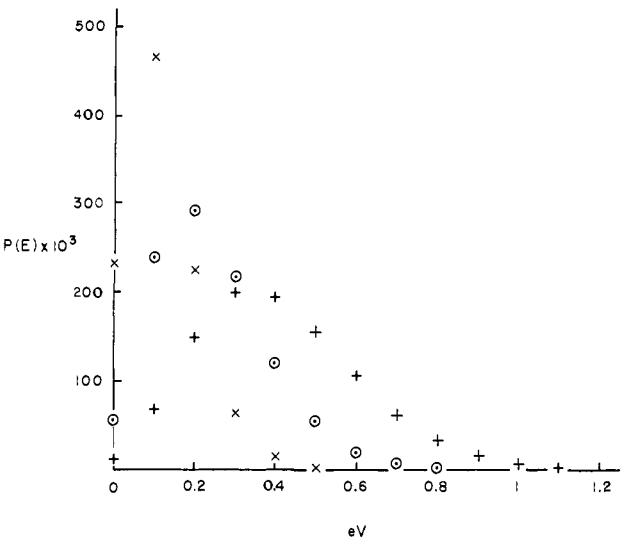

Figure 9. Boltzmann vibrational energy distributions at (×) 298 K, (⊙) 398 K, and (+) 500 K. See text.

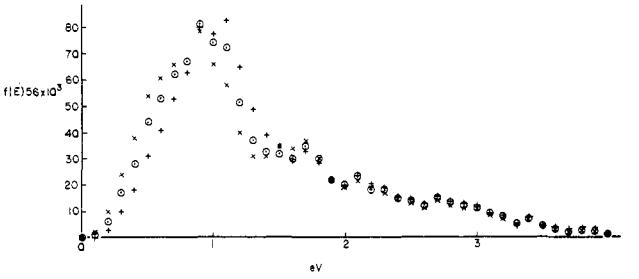

Figure 10. Normalized energy distribution for He Iα photoionized molecular ions which yield m/e 56 at various precursor neutral temperatures. Abscissa represents total energy: (×) 298 K; (⊙) 398 K; (+) 500 K.

As a test of the sensitivity of the calculated distributions to the fundamental frequencies, 500 K Boltzmann distributions were computed by using both the frequencies listed in Table I and an altered set in which the ten lowest frequencies were increased 10%. The average energies of the two distributions differed by only 4% or 0.015 eV. The degeneracies are shown in parentheses in Table I and were assigned based upon structural properties.

Figure 9 exhibits the Boltzmann distributions for 2-butyl acetate at three temperatures important to the results observed on electron impact.[8,13] Note that the room-temperature Boltzmann distribution is relatively narrow. Its peak lies close to its average energy of 0.12 eV. For these reasons as well as to simplify the calculations, the 298 K Boltzmann distribution was approximated as a δ function at 0.1 eV whenever it was necessary to perform a deconvolution. This permits the thermal distribution to be unfolded by merely shifting the energy axis by the average thermal energy.

The convolution integration (1) was then carried out for five temperatures between 298 and 500 K corresponding to the range of Boltzmann distributions exhibited in Figure 9. The adiabatic ionization potential was taken as 9.90 eV. The energy distribution for those molecular ions which produce m/e 56 after He Iα photon ionization can be obtained at each temperature through multiplying the O K breakdown curve for m/e 56 by the $F(E)$ obtained from the convolution integral and normalizing. The measured

(26) Detailed discussions of these points and the procedures may be found in K. Levsen, ref 22, and also W. Forst, "Theory of Unimolecular Reactions", Academic Press, New York, 1973, p 307 ff, Series Editor E. Loebl. The foundations of these ideas and their utilization as well as leading references are found in W. A. Chupka, *J. Chem. Phys.*, **54**, 1936 (1971); **30**, 191 (1959); F. W. McLafferty, T. Wachs, C. Lifschitz, G. Innorta, and P. Irving, *J. Am. Chem. Soc.*, **92**, 6867 (1970); D. J. McAdoo, P. F. Bente, III, M. L. Gross, and F. W. McLafferty, *Org. Mass Spectrom.*, **9**, 525 (1974); P. F. Bente, III, F. W. McLafferty, D. J. McAdoo, and C. Lifshitz, *J. Phys. Chem.*, **79**, 713 (1975).

(27) J. E. Saunders, J. J. Lucier, and F. F. Bentley, *Appl. Spectrosc.*, **22**, 697 (1968). "CRC Atlas of Spectral Data and Physical Constants of Organic Compounds", 2nd ed., J. G. Grasselli and W. M. Ritchey, Eds., 1975. L. J. Bellamy, "The Infra-red Spectra of Complex Molecules", Wiley, New York, 1958.

(28) T. Beyer and D. F. Swinehart, *Commun. ACM*, **16** (June), 379 (1973).

Table II. Calculated Stereoselectivities for Photoionized 2-Butyl Acetate at Various Temperatures

T, K	$\bar{k}_a/\bar{k}_b$	T, K	$\bar{k}_a/\bar{k}_b$
298	1.468	426	1.440
348	1.459	500	1.420
398	1.447		

breakdown curve (Figure 3 (bottom)) was taken at room temperature, and, therefore, as discussed just above, the thermal energy was unfolded by shifting the energy axis by 0.1 eV. The $f(E)_{56}$ so obtained for three precursor neutral temperatures are exhibited in Figure 10.

The three $f(E)_{56}$ distributions corresponding to precursor temperatures of 298, 398, and 500 K (Figure 10) all show structural breaks in correspondence with structural features of the breakdown curve for m/e 56 (Figure 3) as expected from the method of calculation. Consistent with the thermal distributions in Figure 9 which show the energy distribution concentrated below about 1.3 eV in all cases, the temperature effect on $f(E)_{56}$ only makes a difference in the broad ionization region corresponding to the nonbonding promotion in the photoelectron spectrum.[17] The long energy tail reaching to almost 4 eV above onset is unaffected by the temperature change. Thus we can see from inspection of the microscopic stereoselective channel ratios exhibited in Figure 8 that temperature change causes changes in the energy distribution in the area corresponding to the maximum change in k_a/k_b, i.e., from onset to about 1.5 eV above this point. If we were therefore measureing a $\bar{k}_a/\bar{k}_b$ ratio averaged over all energies increasing the temperature can be seen to shift the energy distribution to regions where the microscopic stereoselectivity is lower. This is consistent with the observations in the mass spectrometer.[13]

If one allows utilization of the energy distribution function ($f(E)_{56}$) from the PEPICO experiment, as calculated above, to represent the distribution in the TPEPICO experiment, one could proceed to integrate the microscopic stereoselective channel ratios in Figure 7 over the energy distribution functions of various temperatures (Figure 10) and thereby determine the stereoselectivity weighed over all states which produce acetic acid. In order to carry this out, we first shifted the x axis in Figure 7 by 0.1 eV corresponding to a room temperature δ function deconvolution. This procedure is identical with the procedure used (see above) for the breakdown graph (Figure 3) used in the calculation of $f(E)_{56}$ and causes a correspondence between the energy axes in Figures 7 and 10. The calculation involved separate integration of the microscopic ratio of $k_a/k_a + k_b + k_i$ and of $k_b/k_a + k_b + k_i$ (Figure 7) over the $f(E)_{56}$ for each temperature (Figure 10). The ratios of these integrals are presented in Table II as $\bar{k}_a/\bar{k}_b$.

The first point of interest is the value of 1.47/1 at 298 K because this can be compared with the 1.51/1 ratio of areas under the breakdown graphs for m/e 56 from **1** and **2** (Figure 6). It should be emphasized that both values are derived from the same breakdown graphs (**1** and **2** of Figure 6). However, the ratio 1.47/1 was calculated by numerically integrating the TPEPICO experimental data over the $f(E)_{56}$ distribution obtained from the PEPICO energy deposition function (He Iα photoelectron spectrum used for $D(y)$ in eq 1) and breakdown curve. The near equality of the two ratios serves as a check on both the analytical procedure and the assumptions attendant to the $f(E)_{56}$ distribution.

The $\bar{k}_a/\bar{k}_b$ ratios shown in Table II are sensitive to the experimental data. A change in only the microscopic k_a/k_b at 11 eV from 1.74 to 1.21 (Figure 8) alters the 298 K $\bar{k}_a/\bar{k}_b$ value from 1.47 (Table II) to 1.42/1.

Independent of any experimental uncertainty, the theoretically calculated variation of $\bar{k}_a/\bar{k}_b$ with temperature accurately reflects the shifting of $f(E)_{56}$ to higher energy states with increasing temperature as exhibited in Figure 10. However, the change with temperature predicted for the photoionization process (Table II) is much less than that experimentally determined by electron-impact mass spectrometry.[13] Our knowledge of $f(E)_{56}$ (Figure 10) and the microscopic channel ratios (Figure 8) for the photoionization process points to the onset region, i.e., deposition energies below 10.8 eV, as the source of the difference in the magnitude of the temperature dependency. In this energy region occurs the steepest rise in $f(E)_{56}$ and the steepest descent in k_a/k_b. In computer experiments we have increased the $\bar{k}_a/\bar{k}_b$ temperature dependence, while a linear relationship is maintained with inverse temperature (as found by EI)[13] by simply increasing $f(E)_{56}$ in the region below 0.4 eV.

Table III. Frequency Assignments for 2-Butyl Acetate Fragmentation[a,b]

neutral molecule	model 1	model 2	assignt
281	700	335	torsion
335	rx coord	rx coord	C–O–C bend
353	700	353	
658	1250	600	acetate mode
894	1250	700	C–C rock
1030	1250	1030	C–C stretch
2940	1500	1500	C–H stretch
$\Delta S^{\ddagger}/R$	−3.30	−1.10	
log A factor[c]	12.4	13.36	

[a] All frequencies in cm^{-1}. [b] Only altered frequencies shown. See Table I. [c] Based on the neutral reaction (see ref 5).

The change of $\bar{k}_a/\bar{k}_b$ in the electron impact (EI) mass spectrometer with source temperature[13] is consistent with a monotonic incorporation of thermal energy into the ionization deposited energy and with an increased sampling of microscopic states of lower energy over the photon ionization process. It appears likely, from the present work, that the linearity of the EI temperature dependence may not suggest that the electron-impact produced energy distribution function of molecular ions losing acetic acid is approximately Boltzmann in form.[13]

RRKM Calculations on the Stereoselective Loss of Acetic Acid from Neutral and Ionized 2-Butyl Acetate. In the work below we have attempted to develop an RRKM model consistent with the energy dependence of the microscopic stereoselectivities reported here (Figure 8).

For the ratio of stereoisomeric rates where only one hydrogen each can lead into the stereoisomeric channel the general RRKM equation[29] reduces to eq 2. Q defines rotational partition

$$\frac{k_a(E)}{k_b(E)} = \frac{Q_a^+ G_a^+(E - E_{a0})}{Q_b^+ G_b^+(E - E_{b0})} \tag{2}$$

functions, G designates a sum of states, and E, E_{a0}, and E_{b0} respectively stand for the energy of the reacting molecule and the threshold energies for the stereoisomeric channels. The + sign designates the activated complex. We have assumed that the moments of inertia of the stereoisomeric transition states are equal ($Q_a^+ = Q_b^+$) and further that the transition states are sufficiently similar so that their fundamental frequencies can be taken as identical. This latter assumption is expected to be only slightly in error and results in considerable simplification since only one sum of states as a function of energy need be evaluated. The energy terms are related through eq 3,

$$E = E(\text{deposition}) + \langle E_{\text{thermal}} \rangle - \text{IP} \tag{3}$$

where E is the total internal energy possessed by the ions, E-(deposition) is only that energy deposited in the ionization event (corresponding to the energy axis in Figure 8), and IP is the ionization potential, taken as 9.9 eV. The value for $\langle_{\text{thermal}}\rangle$ was taken as 0.1 eV.

The sum of states function (G^+) appearing in eq 2 is determined by the fundamental frequencies assigned to the transition state (taken to be the same for the stereoisomeric paths, see above). In the case of neutral molecules the transition-state frequencies are established with the constraint that the entropy of activation be identical with that calculated from the experimental Arrhenius

(29) See ref 26 and also P. J. Robinson and K. A. Holbrook, "Unimolecular Reactions", Wiley-Interscience, New York, 1972 for extensive discussions of this theory.

Table IV. RRKM Calculated Microscopic Stereoselective Channel Ratios for Elimination of Acetic Acid from 2-Butyl Acetate

		k_a/k_b(calcd) (eq 2)							
		ΔE_{oab}, cal mol^{-1} ($\Delta S^{\ddagger}/R = -3.30$)				ΔE_{oab}, cal mol^{-1} ($\Delta S^{\ddagger}/R = -1.10$			
E,[a] eV	k_a/k_b(exptl)[b]	400	600	800	1000	400	600	800	1000
0.1	2.72	1.61	2.64	2.64	3.22	1.96	3.06	3.77	4.46
0.2	2.27	1.63	2.04	2.66	3.50	1.65	2.18	2.85	3.70
0.4	2.26	1.45	1.75	2.12	2.56	1.48	1.81	2.21	2.70
0.6	1.73	1.37	1.61	1.89	2.22	1.39	1.64	1.94	2.30
0.8	1.21	1.32	1.52	1.75	2.02	1.34	1.55	1.79	2.08
1.4	1.08	1.24	1.38	1.54	1.72	1.25	1.39	1.56	1.74
1.6	1.65	1.22	1.35	1.50	1.66	1.23	1.36	1.51	1.68
2.8	1.30	1.16	1.25	1.35	1.45	1.16	1.26	1.36	1.46
3.3	1.17	1.15	1.23	1.31	1.40	1.15	1.23	1.32	1.41

[a] $E = E$(deposition) + 0.1 eV − 9.9 eV as per 3. [b] Presented graphically in Figure 8 which also shows the estimated errors in the k_a/k_b values.

preexponential factor. This latter information is available in the reaction where 2-butyl acetate yields the two 2-butene stereoisomers. However the entropy of activation for the decomposition of the 2-butyl acetate ion is unknown.

The decomposition of the ion to yield acetic acid via involvement of the C-3 hydrogen is an example of the McLafferty rearrangement. This well-studied ion process[30] appears to proceed, in analogy to the photochemical reaction,[2,12] via a stepwise mechanism in which the C-3 hydrogen to carbon bond is first broken and the hydrogen becomes bound to the carbonyl oxygen. This step is responsible for the observed stereochemistry. In the neutral reaction there is also a great deal of experimental effort which suggests[2] that the reaction proceeds by partial heterolysis of the C-2 to oxygen bond with partial bonding of the carbonyl oxygen to the C-3 hydrogen. The necessity in both reactions for a six-membered state bringing the acetyl carbonyl and C-3 hydrogen into bonding proximity suggests that the transition states will be described by similar entropies of activation. With this in mind we have carried out an RRKM calculation for the ion utilizing the entropy of activation of the neutral.[31] In addition we have also carried out this calculation at one third the entropy of activation of the neutral. The fundamental frequencies of the ion were taken as identical with those of the neutral molecule in calculating the entropy of activation. The adjusted frequencies in the transition-state model which lead to the chosen entropy of activation are presented in Table III.

The sum of states function (G^+) was calculated by using the direct count algorithm of Beyer and Swinehart[28] with the frequencies listed in Tables I and III. The microscopic stereoselective channel ratio (k_a/k_b) was obtained from eq 2 as the ratio of $G^+(E - E_{a0})$ to $G^+(E - E_{b0})$.

The results of the RRKM calculations of the microscopic stereoselective channel ratios (k_a/k_b) using these models (Table III) are presented in Table IV for nine energies. Comparable experimental data are included for comparison.

From Table IV it may be seen that the RRKM channel ratios for a threshold energy difference of 400 cal/mol fall well below the experimental ratios for all energies less than 0.8 eV. Also the calculated k_a/k_b ratios for a threshold energy difference of 1000 cal/mol lies almost uniformly above the experimental values. The threshold differences of 600 and 800 cal/mol^{-1} both show a general correspondence with the experimental data. Figure 11 shows the graphical representation of the RRKM channel ratios for both 600 and 800 cal/mol^{-1} ΔE_{oab} for the transition-state model based upon the same entropy of activation as the thermal reaction, i.e., $\Delta S^{\ddagger}/R = -3.30$. Comparison of Figure 11 with the experimental values in Figure 8 shows the experimental data scattering evenly about the theoretical line.

The data in Table IV also indicate the RRKM channel ratios are sensitive to the adopted entropy of activation, i.e., the transition-state frequency assignments, only within a few tenths of 1 eV of threshold. The quality of the experimental data in this energy region is not adequate to choose between these models.

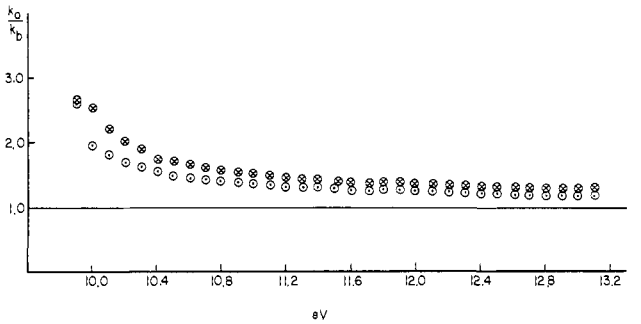

Figure 11. RRKM-derived microscopic stereoselective channel ratios using $\Delta S^{\ddagger}/R = -3.30$ for the 2-butyl acetate ion reaction. ΔE_{oab}, cal mol^{-1}: 600 (⊙); 800 (⊛). See text. Abscissa is plotted as for Figure 8 for ease of comparison: e.g., 0.1 eV from Table 4 corresponds to 9.9 eV in Figures 11 and 8.

The threshold energy difference associated with decomposition of the neutral molecule may be estimated from published thermal stereoselectivity data if the assumption is made that pathways a and b, i.e., formation of *trans*- and *cis*-2-butene, have identical preexponential factors. Emovon and Maccoll[3] measured a $\bar{k}_a/\bar{k}_b$ ratio of 1.78 at 604 K. Skell and Hall[6] found this ratio to be 1.86 at 673 K. These findings imply threshold energy differences of 690 and 830 cal/mol, respectively. Hence, the present results show the threshold energy difference for the ion reaction, as given by the data of Table IV, to be comparable to the threshold energy difference in the reaction of the neutral molecule.

We have taken the RRKM rate constants for the neutral molecule, i.e., from model 1 (Table III), and averaged these values (Table IV) over the appropriate Boltzmann energy distribution to give $\bar{k}_a/\bar{k}_b$ ratios in agreement with Emovan and Maccoll[3] at 604 K with ΔE_{oab} of 700 cal/mol^{-1} and with Skell and Hall[6] at 673 K with ΔE_{oab} of 800 cal/mol^{-1}. This lends strength to the consistency of the experimental thermal data and confidence to the differences in threshold energy of 700–800 cal/mol^{-1} for the stereoisomeric pathways in the neutral molecule.

In the mass spectrum of C-3 dideuterio-2-butyl acetate (**3**) the loss of methyl appears at M − 15, the loss of ethyl at M − 31, and the acetyl group at m/e 43 without any evidence that the deuterium atoms have interchanged their position with hydrogens on other carbons. Nevertheless the occurrence of such scrambling pathways is known to increase in the lowest energy ions and therefore be most competitive with rearrangement reactions[32] such as the process producing acetic acid loss studied here. In the study of stereoselectivity, scrambling need not change the positions of hydrogens but rather the simple reversibility of the step in which hydrogen transfers from C-3 to the acetate group would allow

(30) For the most recent discussion and leading references see: K. Levsen in ref 22, pp 194–196.

(31) See W. Forst in ref 26, p 364, for this argument and also for general support for this approach in evaluating the entropy of activation in the ion reaction.

(32) See K. Levsen in ref 22 for an excellent discussion of this area and leading references: p 98 ff and 186 ff.

epimerization of C-3 and therefore cause **1** and **2** to lose their stereochemical identity. We have measured the metastable peak intensities for loss of DO_2CCH_3 and HO_2CCH_3 from **1** and **2** and find no difference.[33] This result suggests that a scrambling mechanism is effectively competing with acetic acid loss under the conditions for metastable ion formation in the electron-impact mass spectrometer.[33] Scrambling competition should increase as the energy decreases, and therefore the rise in the microscopic channel ratios (k_a/k_b) with decreasing energy (Figure 8, Table IV) suggests that such a process is not intervening here. Nevertheless we have no firm evidence to totally exclude a mechanism which may partially interconvert **1** and **2**, and therefore the RRKM derived values of ΔE_{oab} which best match our experimental results must be taken at present, as minimum values.[35] Note the contrast, that in the thermal reaction of the neutral molecule[2] the fact that each diastereotopic deuterium is incorporated specifically into one stereoisomeric 2-butene[6] does not allow any intermediate states which mix the paths to *cis*- and *trans*-2-butene from **1** and **2**.

The literature concerned with the mechanism of the compared ion and thermal reaction for acetic acid loss from 2-butyl acetate[2,30] suggests that these processes share the essential transition-state features of proximity between the C-3 hydrogen and the acetyl carbonyl oxygen and the absence of double-bond character between C-2 and C-3. The resulting necessary conformational states would cause, in both the ion and the thermal reaction, a methyl methyl and a hydrogen hydrogen eclipsing strain in the loss of H_b, i.e., the cis pathway (k_b), and two methyl hydrogen eclipsing interactions leading to loss of H_a, i.e., the trans pathway (k_a). It follows from these considerations that the steric energy difference between the pathways for loss of the C-3 diastereotopic hydrogens should be similar, as we find here, in the compared ion and thermal reactions.[36]

Experimental Section

The C-3 deuterated racemic diastereomers of 2-butyl acetate (**1** and **2**) were prepared as described.[6,8] The C-3 dideuterio-2-butyl acetate (**3**) was prepared by reduction of acetic acid to 1,1-dideuterioethanol, conversion to 1,1-dideuterioethyl bromide, and Grignard reaction with acetyldehyde. The resulting 3,3-dideuterio-2-butanol was esterified with acetic anhydride and collected by preparative gas chromatography. The three deuterated materials were by gas chromatography identical with each other and with 2-butyl acetate standard and were at least 99% homogenious.

The coincidence experiments were conducted on the PEPICO and TPEPICO instruments which have been described.[15,16]

The calculations were carried out on an IBM System 360 Model 65 computer, and the programs are available from R.J.M.

Acknowledgment. Work at the Polytechnic Institute and Clarkson College was financially supported by grants from the National Institutes of Health General Medical Sciences and the donors of the Petroleum Research Fund, administered by the American Chemical Society, to whom we are grateful. Work at the Physikalisch Chemisches Institut has been supported by the Schweizerischer Nationalfounds zur Förderung der Wissenschaftlichen Forschung, Part C-17 of Project No. 2.212-0.79. Financial support by Ciba-Geigy SA, Hoffman-LaRoche & Cie SA, and Sandoz SA, Basel, is gratefully acknowledged. We are indebted to Drs. H. Rosenstock, A. Parr, R. Stockbauer, and E. White V. for their help with experiments conducted on equipment at the National Bureau of Standards and to Professor Tomas Baer for helpful comments.

Registry No. (±)**1**, 56552-75-1; (±)**2**, 56552-76-2; **3**, 80846-06-6; 2-butyl acetate ion, 80846-07-7; 2-butyl acetate, 105-46-4; acetic acid, 64-19-7.

(33) Unpublished data taken by Dr. E. White V. at the National Bureau of Standards, Washington, D.C., in the field free region of a Varian Finnigan MAT731 mass spectrometer.

(34) The stereoselectivity for the normal electron-impact produced ions increases with decreased temperature at about 70 eV and near the ionization threshold[13] and therefore offers no evidence of scrambling. Similar high specificity has been found by R. N. Rej, E. Bacon, and G. Eadon, *J. Am. Chem. Soc.*, **101**, 1668 (1979). There is precedence for nonspecificity in elimination reactions to intervene in metastable but not normal ions. See: P. J. Derrick, J. L. Holmes, and R. P. Morgan, *ibid.*, **97**, 4936 (1975) and references therein.

(35) Increasing the lifetime and/or decreasing the energy of the *m/e* 56 producing molecular ions in the coincidence spectrometer to find where k_a/k_b falls back toward unity could be one way of detecting the onset of stereochemical scrambling.

(36) This work further supports the utility of stereochemical observations for relating gas phase ion chemistry and the chemistry of thermalized molecules as discussed in: M. M. Green, *Tetrahedron*, **36**, 2687 (1980), Report No. 95.

Stereochemical Aspects of the Intramolecular Diels–Alder Reactions of Deca-2,7,9-trienoate Esters. 3. Thermal, Lewis Acid Catalyzed, and Asymmetric Cyclizations

William R. Roush,* Herbert R. Gillis, and Albert I. Ko

Contribution from the Department of Chemistry, Massachusetts Institute of Technology, Cambridge, Massachusetts 02139. *Received July 16, 1981*

Abstract: Stereochemical aspects of the intramolecular Diels–Alder reactions of a series of deca-2,7,9-trienoate esters are described. The thermal cyclizations of trienes **4–8** afforded mixtures of cycloadducts, among which the trans-fused products predominated. The product selectivity in these cases was independent of dienophile stereochemistry. The structures of the cycloadducts were established by chemical methods, including product interconversions, degradations, and independent synthesis. The cyclizations of **5–8** were catalyzed by a number of Lewis acids, of which ethylaluminum dichloride, diethylaluminum chloride, and (menthyloxy)aluminum dichloride were particularly effective. The Lewis acid catalyzed cyclizations of **5** and **7** afforded trans-fused products, exclusively, in excellent yield, whereas the catalyzed cyclizations of **6** and **8** afforded mixtures of cycloadducts in poor yield. The catalyzed cyclizations of chiral triene esters **61** and **62** afforded mixtures of trans-fused diastereomeric products, the diastereomeric excess (corresponding to enantiomeric excess) of which, in most cases, ranged from 30% (for **61**) to 64% (for **62**).

The intramolecular Diels–Alder reaction promises to become widely used in the synthesis of natural products.[1] The reaction has been used to synthesize a number of interesting ring systems and has already been applied to a variety of problems in natural

0002-7863/82/1504-2269$01.25/0